Dynamic Response Of Deeply Embedded Shafts

L.E. Pérez, L.E. Manjarrez, M.A. Fernández & D. Maldonado
Instituto de Investigaciones Eléctricas, Cuernavaca, Morelos, México.

J. Avilés
Instituto Mexicano de Tecnología del Agua, Cuernavaca, Morelos, México

SUMMARY:
A boundary method to analyze the dynamic soil-shaft interaction considering the flexibility of the structure and the translation-rotation of its base is presented. The model consists in a floating flexible cylinder embedded in a soil deposit with rigid base, forming two regions: one interior including the shaft and the supporting soil and another exterior including the surrounding soil. For each region, displacements and forces are expressed by means of superposition of wave modes traveling horizontally. Boundary conditions in the interface between the two regions given by the compatibility of displacements and forces are imposed at nodal points. Vertical incidence of shear waves is considered as excitation of the system. In both regions, wave modes are computed with the finite layer method, in such a way that the solution is discreet in the vertical direction and continuous in the horizontal one. The application and accuracy of this method is illustrated with some examples reported in the specialized literature.

Keywords: Soil-shaft interaction, floating, supported, fixed, thin layer method, shear force, bending moment.

1. INTRODUCTION

Seismic effects in underground structures are often evaluated with different approaches to the ones employed for surface structures. In general, for underground structures design actions are expressed in terms of displacements and deformations imposed in the structure by the soil as a result of the interaction between them. The simplest design approach is the one ignoring the interaction of the underground structure with the surrounding soil. According to this approach, first the free field ground deformations are estimated, and then the structure is designed to be adjusted to these deformations. The result is reasonable when the soil is much more rigid than the structure. On the contrary, it is necessary to consider dynamic interaction effects, since they can affect the surrounding deformations considerably. These effects are due to the wave diffraction produced by the structure (kinematic interaction), as well as to the inertial forces generated by the vibration of the system (inertial interaction).

During earthquakes, shafts are subjected to significant curvatures imposed by the lateral ground motion. Such curvatures generate important bending moments. Solutions reported in the literature are scarce and limited. The approximated solution of Veletsos y Younan (1994; 1995) is remarkable because of its simplicity and attractiveness. It is based on the hypothesis of null vertical (normal) stresses. This idealization of the soil was proposed by Arias et al (1981) to compute dynamic pressures in retaining walls. The solution of Veletsos and Younang is superior to the one of Tajimi (1969) based on the hypothesis of null vertical displacements. Both solutions, however, are applicable to rigid structures with fixed base. For these conditions, the resulting soil actions are excessively great with respect to the ones corresponding to floating flexible shafts. The flexibility of the structure and the translation-rotation of its base produce a remarkable reduction of these actions. This effect has been studied by Nicolau et al (2001) in piles of great dimensions by using an approximated model of a beam on a Winkler elastic foundation.

A boundary method for seismic analysis of soil-shaft systems, regarding the flexibility of the walls and the floating of the bottom, is described in what follows. The model consists in an elastic cylinder embedded in a soil deposit with rigid base forming two regions: one interior with the shaft and the supporting soil, and the other exterior with the surrounding soil. For each region, the displacements and forces are expressed by means of a superposition of wave modes with horizontal propagation. Then, boundary conditions are imposed in the interface between both regions, given by compatibility of displacements and forces. Vertical incidence of shear waves is considered as excitation. Thin layer method is used to compute wave modes in both regions, in such a way that the solution is discrete in the vertical direction and continuous in the horizontal one.

2. FORMULATION OF THE PROBLEM

2.1. Equations of motion

Soil-shaft system is composed by a shaft of radius r_o embedded in a horizontally layered soil deposit. Each layer has thickness h_j, shear wave velocity $\beta_j = \sqrt{G_j/\rho_j}$, being G_j the shear modulus and ρ_j the mass density, damping ζ_j and Poisson ratio υ_j. Let be u, v and w the radial, tangential and axial displacements, respectively, in cylindrical coordinates (r,θ,z) where vertical coordinate grows with depth. If the soil deposit is divided in N layers, the differential equations that govern the harmonic motion in the $1 < j < N$ layer are

$$\nabla^2 u - \frac{u}{r^2} - \frac{2}{r^2}\frac{\partial v}{\partial \theta} + \frac{1}{1-2\upsilon_j}\frac{\partial \varepsilon}{\partial r} + \frac{\omega^2}{\beta_j^2} u = 0 \tag{2.1}$$

$$\nabla^2 v - \frac{v}{r^2} - \frac{2}{r^2}\frac{\partial u}{\partial \theta} + \frac{1}{1-2\upsilon_j}\frac{1}{r}\frac{\partial \varepsilon}{\partial \theta} + \frac{\omega^2}{\beta_j^2} v = 0 \tag{2.2}$$

$$\nabla^2 w + \frac{1}{1-2\upsilon_j}\frac{\partial \varepsilon}{\partial z} + \frac{\omega^2}{\beta_j^2} w = 0 \tag{2.3}$$

where ω is the frequency of excitation, υ_j is the Poisson ratio and $\beta_j = \sqrt{G_j/\rho_j}$ is the shear wave velocity, being G_j the shear modulus and ρ_j the mass density; ∇^2 and ε are the Laplacian and the expansion (dilatación), respectively, defined as

$$\nabla^2 = \frac{\partial^2}{\partial r^2} + \frac{1}{r}\frac{\partial}{\partial r} + \frac{1}{r^2}\frac{\partial^2}{\partial \theta^2} + \frac{\partial^2}{\partial z^2} \tag{2.4}$$

$$\varepsilon = \frac{\partial u}{\partial r} + \frac{1}{r}\left(u + \frac{\partial v}{\partial \theta}\right) + \frac{\partial w}{\partial z} \tag{2.5}$$

Let be $\lambda_j = 2\upsilon_j G_j/(1-2\upsilon_j)$ the constant of Lamé. Stress components over a cylindrical surface are related with displacement components by means of:

$$\sigma_r = \lambda_j \varepsilon + 2G_j\frac{\partial u}{\partial r}, \quad \tau_{rz} = G_j\left(\frac{\partial u}{\partial z} + \frac{\partial w}{\partial r}\right), \quad \tau_{r\theta} = G_j\left(\frac{\partial v}{\partial r} - \frac{v}{r} + \frac{1}{r}\frac{\partial u}{\partial \theta}\right) \tag{2.6}$$

2.2. Azimuthal decomposition

Axial symmetry of the structure allows carrying out an azimuthal decomposition of the solution. According to Kausel and Roësset (1975 and 1977), modal displacements (radial, vertical and tangential) can be obtained by separation of variables as is indicated.

Rayleigh generalized modes in plane deformation

$$u(r,\theta,z) = \bar{u}(r,z)\begin{Bmatrix} cos\, n\theta \\ \mathrm{sen}\, n\theta \end{Bmatrix}, \text{ con } \bar{u} = kU(z)C_n'(kr) \tag{2.7}$$

$$w(r,\theta,z) = \bar{w}(r,z)\begin{Bmatrix} cos\, n\theta \\ \mathrm{sen}\, n\theta \end{Bmatrix}, \text{ con } \bar{w} = -ikW(z)C_n(kr) \tag{2.8}$$

$$v(r,\theta,z) = \bar{v}(r,z)\begin{Bmatrix} -\mathrm{sen}\, n\theta \\ \cos n\theta \end{Bmatrix}, \text{ con } \bar{v} = \frac{n}{r}U(z)C_n(kr) \tag{2.9}$$

Love generalized modes in antiplane shear

$$u(r,\theta,z) = \bar{u}(r,z)\begin{Bmatrix} cos\, n\theta \\ \mathrm{sen}\, n\theta \end{Bmatrix}, \quad \text{con } \bar{u} = \frac{n}{r}V(z)C_n(kr) \tag{2.10}$$

$$w(r,\theta,z) = 0 \tag{2.11}$$

$$v(r,\theta,z) = \bar{v}(r,z)\begin{Bmatrix} -\mathrm{sen}\, n\theta \\ \cos n\theta \end{Bmatrix}, \text{ con } \bar{v} = kV(z)C_n'(kr) \tag{2.12}$$

where k is the horizontal wave number and n is the azimuthal wave number; $C_n(\xi)$ is a solution of the Bessel equation of n-order, given by

$$C_n'' + \frac{1}{\xi}C_n' + \left(1 - \frac{n^2}{\xi^2}\right)C_n = 0 \tag{2.13}$$

The time harmonic factor $e^{i\omega t}$ has been omitted by simplicity. For symmetrical modes with respect to plane $\theta = 0$, $\bar{u}$ and $\bar{w}$ are combined with $cos\, n\theta$ and $\bar{v}$ with $-sin\, n\theta$. On the contrary, $\bar{u}$ and $\bar{w}$ are combined with $sin\, n\theta$ and $\bar{v}$ with $cos\, n\theta$ for antisymetrical modes. Replacing Eqns 2.7-2.12 in stress components given in Eqn 2.6, can be verified that

$$\sigma_r(r,\theta,z) = \bar{\sigma}_r(r,z)\begin{Bmatrix} cos\, n\theta \\ \mathrm{sen}\, n\theta \end{Bmatrix}, \quad f_r(r,\theta,z) = \int \sigma_r(r,\theta,z)dz = \bar{f}_r(r,z)\begin{Bmatrix} cos\, n\theta \\ \mathrm{sen}\, n\theta \end{Bmatrix} \tag{2.14}$$

$$\tau_{rz}(r,\theta,z) = \bar{\tau}_{rz}(r,z)\begin{Bmatrix} cos\, n\theta \\ \mathrm{sen}\, n\theta \end{Bmatrix}, \quad f_z(r,\theta,z) = \int \tau_{rz}(r,\theta,z)dz = \bar{f}_z(r,z)\begin{Bmatrix} cos\, n\theta \\ \mathrm{sen}\, n\theta \end{Bmatrix} \tag{2.15}$$

$$\tau_{r\theta}(r,\theta,z) = \bar{\tau}_{r\theta}(r,z)\begin{Bmatrix} -\mathrm{sen}\, n\theta \\ \cos n\theta \end{Bmatrix}, \quad f_\theta(r,\theta,z) = \int \tau_{r\theta}(r,\theta,z)dz = \bar{f}_\theta(r,z)\begin{Bmatrix} -\mathrm{sen}\, n\theta \\ \cos n\theta \end{Bmatrix} \tag{2.16}$$

where $\bar{f}_r(r,z) = \int \bar{\sigma}_r(r,z)dz$, $\bar{f}_z(r,z) = \int \bar{\tau}_{rz}(r,z)dz$ and $\bar{f}_\theta(r,z) = \int \bar{\tau}_{r\theta}(r,z)dz$. These forms show that azimuthal decomposition of stresses and forces is identical to the one of displacements. Azimuthal function $\cos n\theta$ or $\sin n\theta$ selection depends on the physics of the problem. For horizontal excitation x_g, their components in cylindrical coordinates are $u_g = x_g \cos\theta$, $w_g = 0$ and $v_g = -x_g \sin\theta$. Note that the analysis of symmetrical vibrations just requires the azimuthal number $n = 1$. Thus, the three-dimensional problem is reduced to a two - dimensional one in the plane $r - z$.

2.3. Boundary conditions

In order to solve the interaction problem, spatial domain is divided in two regions: 1) one interior i ($r \le r_o, 0 \le z \le H_s$) for the shaft and the supporting soil and 2) another exterior e ($r \ge r_o, 0 \le z \le H_s$) for the surrounding soil, being r_o the radius of the shaft and H_s the depth of the soil deposit. Exterior region is formed only by soil layers, whereas the interior is formed by layers of both, shaft and soil. To satisfy conditions of compatibility in the interface between regions, the method of nodal points collocation is used. In each region, fields of nodal displacement and forces can be built by superposition of the free field and a diffracted field as follows:

$$\tilde{\delta}_\varepsilon = \tilde{\delta}^f_\varepsilon + \tilde{\delta}^d_\varepsilon = \tilde{\delta}^f_\varepsilon + \tilde{\Delta}_\varepsilon \tilde{C}_\varepsilon, \quad \varepsilon = i, e \tag{2.17}$$

$$\tilde{f}_\varepsilon = \tilde{f}^f_\varepsilon + \tilde{f}^d_\varepsilon = \tilde{f}^f_\varepsilon + \tilde{F}_\varepsilon \tilde{C}_\varepsilon, \quad \varepsilon = i, e \tag{2.18}$$

where:

$\tilde{\delta}^f_\varepsilon$	=	vector of free field displacements in ε
$\tilde{f}^f_\varepsilon$	=	vector of free field forces in ε
$\tilde{\delta}^d_r$	=	vector of diffracted displacements in ε
$\tilde{f}^d_\varepsilon$	=	vector of diffracted forces in ε
$\tilde{\Delta}_\varepsilon$	=	matrix of modal displacements in ε
$\tilde{F}_r$	=	matrix of modal forces in ε
$\tilde{C}_\varepsilon$	=	vector of coefficients of participation in ε

Boundary conditions that must be satisfied in the interface between regions are the compatibility of nodal displacements and forces, that is

$$\tilde{\delta}_e(r_o, z_j) = \tilde{\delta}_i(r_o, z_j), \quad 1 \le j \le N \tag{2.19}$$

$$\tilde{f}_e(r_o, z_j) = \tilde{f}_i(r_o, z_j), \quad 1 \le j \le N \tag{2.20}$$

Replacing Eqs 2.17 and 2.18 in Eqs 2.19 and 2.20, respectively, next matrix system of algebraic equations is obtained

$$\left[\begin{array}{c|c} \tilde{\Delta}_e(r_o, z_j) & -\tilde{\Delta}_i(r_o, z_j) \\ \hline \tilde{F}_e(r_o, z_j) & -\tilde{F}_i(r_o, z_j) \end{array}\right] \left\{\begin{array}{c} \tilde{C}_e \\ \hline \tilde{C}_i \end{array}\right\} = \left\{\begin{array}{c} \tilde{\delta}^f_i(r_o, z_j) - \tilde{\delta}^f_e(r_o, z_j) \\ \hline \tilde{f}^f_i(r_o, z_j) - \tilde{f}^f_e(r_o, z_j) \end{array}\right\}, \; 1 \le j \le N \tag{2.21}$$

Solving this equation system with a standard Gaussian elimination method, coefficients of participation that define the nodal displacements and forces fields in both regions are obtained.

3. NUMERICAL IMPLEMENTATION

3.1. Diffracted fields

By appliying the thin layer method (Lysmer y Waas, 1972; Lysmer y Drake, 1972), it is easy to demonstrate that the discrete eigenfunctions $U(z_j)$ and $W(z_j)$ with eigenvalue *k* that satisfy the equations of motions in plane deformation, the continuity of stresses and displacements between layers condition and free surface and rigid base boundary conditions, are obtained by solving the algebraic problem of characteristic values.

$$\left[k^2\tilde{A} + ik\tilde{B} + \tilde{G} - \omega^2\tilde{M}\right]\tilde{\Lambda} = \tilde{0}\,;\ \text{ where } \tilde{\Lambda} = \left\{\Lambda_{2j-1} = U_j,\quad \Lambda_{2j} = W_j\right\}^T,\quad 1 \le j \le N \tag{3.1}$$

is an eigenvector of nodal amplitudes and $\tilde{A}$, $\tilde{B}$, $\tilde{G}$ and $\tilde{M}$ are matrices of $2N \times 2N$ assembled with layer matrices for plane deformations elements (Tassoulas y Kaussel, 1983). After solving Eqn. 3.1 it is necessary to select the values of k_l and $\tilde{\Lambda}_l$, $1 \le l \le 2N$, such that modal displacements in exterior region decay with distance. In order to fulfill this condition of radiation, it is required that $\mathrm{Im}\left[k_l\right] < 0$.

Also it is easy to demonstrate that discrete eigenfunction $V(z_j)$ with eigenvalue k that satisfies the equation of motion in antiplane shear, continuity of stresses and displacements between layers condition and free surface and rigid base boundary conditions, are obtained by solving the algebraic problem of characteristic values

$$\left[k^2\tilde{A} + \tilde{G} - \omega^2\tilde{M}\right]\tilde{\Lambda} = \tilde{0}\,;\ \text{ where } \tilde{\Lambda} = \left\{\Lambda_j = V_j\right\},\quad 1 \le j \le N \tag{3.2}$$

is an eigenvector of nodal amplitudes and $\tilde{A}$, $\tilde{G}$ and $\tilde{M}$ are matrices of $N \times N$ assembled with the layer matrices for antiplane shear elements (Tassoulas y Kaussel, 1983). After solving Eqn. 3.2 it is necessary to select the values of k_l and $\tilde{\Lambda}_l$, $1 \le l \le N$, such that modal displacements in the exterior region decay with distance. In order to fulfill this condition of radiation, it is required that $\mathrm{Im}\left[k_l\right] < 0$.

Once solved the problems of characteristic values in plane deformation and antiplane shear, matrices of modal displacements and modal forces in the cylindrical surface $r = r_o$ can be built following the expressions provided by Kausel and Roësset (1975 y 1977) and Tassoulas and Kaussel (1983).

$$\tilde{\Delta}_\varepsilon = \left[\Delta_{3j-2,l} = \bar{u}_l(r_o, z_j),\ \ \Delta_{3j-1,l} = \bar{w}_l(r_o, z_j),\ \ \Delta_{3j,l} = \bar{v}_l(r_o, z_j)\right]^T,\ 1 \le j \le N \ \text{ y } \ 1 \le l \le 3N \tag{3.3}$$

where:

$$\Delta_{3j-2,l} = k_l U_j^l C_n'(k_l r_o),\quad \Delta_{3j-1,l} = -ik_l W_j^l C_n(k_l r_o),\quad \Delta_{3j,l} = \frac{n}{r_o} U_j^l C_n(k_l r_o) \quad \text{if } 1 \le l \le 2N \tag{3.4}$$

$$\Delta_{3j-2,l} = \frac{n}{r_o} V_j^{l-2N} C_n(k_l r_o),\quad \Delta_{3j-1,l} = 0,\quad \Delta_{3j,l} = k_l V_j^{l-2N} C_n'(k_l r_o) \quad \text{if } 2N+1 \le l \le 3N \tag{3.5}$$

The eigenvalues $k_1,\ldots,k_{2N}$ and $k_{2N+1},\ldots,k_{3N}$ correspond to Rayleigh and Love generalized modes, respectively. Hankel function of second specie and order *n*, $C_n(\xi) = H_n^2(\xi)$, must be used for wave radiation in exterior region. As well, Bessel function of first specie and order *n*, $C_n(\xi) = J_n(\xi)$, must be used for steady waves in the interior region.

Nodal forces acting in the cylindrical surface $r = r_o$ can be obtained by integrating the corresponding stresses with respect to *z*. This discretized forces are in static equilibrium with the layer stresses and are consistent with the considered linear interpolation of displacements. Kausel and Roësset (1975 y 1977) and Tassoulas and Kaussel (1983) provide expressions to construct the matrix of nodal forces.

3.2. Free fields

Free field displacements due to vertical incidence of shear waves, in cylindrical coordinates, are expressed as

$$u(r,\theta,z) = \bar{u}(r,z)\,cos\,\theta, \quad w(r,\theta,z) = 0, \quad v(r,\theta,z) = -\bar{v}(r,z)\,\mathrm{sen}\,\theta \tag{3.16}$$

with $\bar{u}(r,z) = \bar{v}(r,z) = V(z)$. Following Tassoulas and Kausel formulation (1983) for vertical propagation, $k = 0$, nodal amplitudes $V(z_j)$ are obtained from the algebraic equation system

$$\left[\tilde{G} - \omega^2 \tilde{M}\right]\tilde{V} = \tilde{0} \tag{3.17}$$

where $\tilde{V} = \left\{V_j\right\}$, $1 \le j \le N+1$. To solve it is necessary to impose $V_{N+1} = x_g$ at the base, eliminating the last row-column of the matrices $\tilde{G}$ and $\tilde{M}$ and the last element of the vectors $\tilde{V}$ and $\tilde{0}$.

Finally, with free field displacements

$$\tilde{\delta}_\varepsilon^f = \left\{\delta_{3j-2} = V_j, \ \delta_{3j-1} = 0, \ \delta_{3j} = V_j\right\}^T, \quad 1 \le j \le N \tag{3.18}$$

free field forces are obtained

$$\tilde{f}_\varepsilon^f = \tilde{D}\,\tilde{\delta}_\varepsilon^f \tag{3.19}$$

where $\tilde{D}$ is the matrix used in Eqn 3.8, multiplying columns $3j-1$ by -1. Due to the structure of this matrix, radial and tangential forces are null for horizontal excitation.

3.3. Shear force and bending moment

Given the nodal forces $\bar{f}_r^j$ y $\bar{f}_\theta^j$ in the cylindrical surface $r = r_o$, the resultant force in lateral direction is determined by integration with respect to θ:

$$F_x^j = \int_0^{2\pi} (\bar{f}_r^j\,cos^2\theta + \bar{f}_\theta^j\,\mathrm{sen}^2\theta)\,r_o\,d\theta = \pi r_o (\bar{f}_r^j + \bar{f}_\theta^j), \quad 1 \le j \le N \tag{3.20}$$

The resultant force in vertical direction is null. Note that the shear and normal nodal forces contribute in the same proportion to the lateral thrust. Once lateral forces are known, shear force Q_z and bending moment M_z at z level can be computed by simple static.

4. NUMERICAL RESULTS

4.1. Example 1: Comparison with Veletsos and Younan

Analytical solution of Veletsos and Younan (1994; 1995) was considered for this example corresponding to a rigid cylinder fixed at the base of an homogeneous layer. For harmonic excitation of the basement, static values of base shear force bending moment. Shear force $\widetilde{Q}_o$ and bending moment $\widetilde{M}_o$ are normalized with respect to $\pi r_o \rho_s \ddot{x}_g H_o^2$ and $\pi r_o \rho_s \ddot{x}_g H_o^3$, respectively, where $\ddot{x}_g$ denotes the peak ground acceleration at rock. Static values correspond to a harmonic excitation with frequency much smaller than the fundamental frequency of the layer. Resultant effects do not have to be confused with the effects due to gravitational loads. In the equivalent version of the system with fixed base, the static excitation is represented by lateral body forces with intensity $-\rho_s \ddot{x}_g$ for the soil and $-\rho_o \ddot{x}_g$ for the structure. Figure 1 shows the variation of base shear force and bending moment with respect to the slenderness ratio, H_o/r_o, for a soil deposit with $\nu_s = 0$, 1/3 y 1/2, and $\zeta_s = 0.05$.

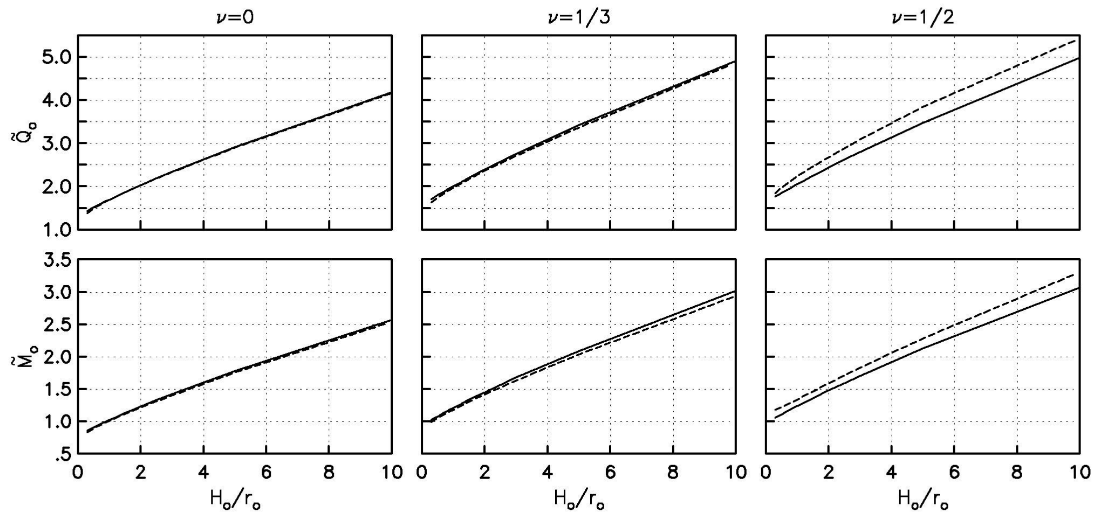

Figure 1. Comparison of static values of base shear force and bending moment numerically obtained (dashed lines) versus analytical results (solid lines), for $\nu_s = 0$ (left), $\nu_s = 1/3$ (center), $\nu_s = 1/2$ (right).

Comparison of numerical and analytical results shows an excellent agreement, especially when the Posson ratio is not close to 0.5. In this case, analytical solution present differences due to a strong hypothesis consisting in neglecting the vertical component of the motion. For this reason, the analytical solution is susceptible when $\nu_s = 1/2$.

4.2. Example 2: Comparison with Nicolau et al.

Analytical solution of Nicolau et al (2001) was considered for this example. This one is based on an approximated model of beam on elastic foundation. The geotechnical model of the soil consists in two layers. For the resonant frequency, $\omega = \omega_1$, the case of an embedded pile in a soil deposit formed by two layers with rigid base is analyzed. Parameters of the system are: $L/d = 20$, $E_p/E_1 = 1000$, $h_1/L = 2/3$, $h_1/L = 1$, $V_1/V_2 = 1/2$, $\rho_1/\rho_2 = 0.8$, $\nu_1 = \nu_2 = 0.4$ and $\zeta_1 = \zeta_2 = 0.1$. Here L is the length of the pile, d is the diameter of the pile, E_p and E_1 are the elasticity module of pile and soil, respectively, h_1 is the thickness of the top layer, h_3 is the distance between the base of the pile and the base of the bottom layer, V, ρ, ν and ζ are the shear wave propagation velocity, mass density, Poisson ratio and damping, respectively. Subindex 1 and 2 indicate top and bottom layers, respectively. Bending deformation computed by Nicolay et al (2001) is related with bending moment by means of

$$\varepsilon_p = \frac{M}{E_p I_p} \frac{d}{2} \tag{4.1}$$

Comparison of bending deformation and bending moment against the computed values using the developed method are shown in Figure 2. Major difference is observed in the base of the pile, and it is due to the boundary condition used. Free stress support has been considered when, in fact, a displacement and force compatibility condition is had.

Note that the Nicolau et al (2001) method is approximated, since the soil-pile system is modeled as a beam on elastic foundation. In order to consider the continuity condition at the base, it is necessary to include translational and rotational springs substituting the supporting soil instead of the free stress support. Difficultness to do that relies on the nature of the expressions of such springs, since they correspond to superficial discs, disregarding the depth of foundation effect.

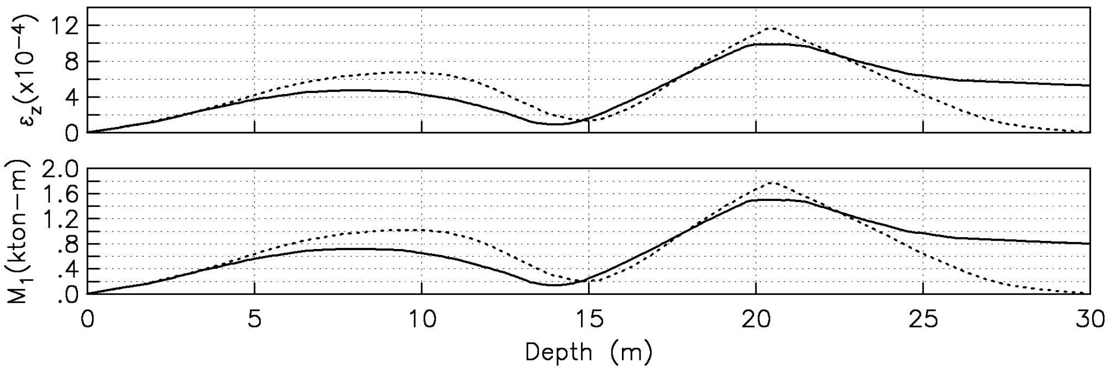

Figure 2. Comparison of bending deformations and moments along the pilot computed with the Nicolau et al (2001) method (dashed line) and this method (solid line)

4.3. Example 3: Comparison with Zeevaert

In case of supported pilots in a hard layer, it can be supposed that the pilot is articulated at the end. However, in case of same supported piles, and considering these foundation elements are quite rigid due to their great diameter, the restriction of rotation of the supporting base is very important in the interaction analysis. The reason is because the moment developed there is proportional to the size of the base and to the stiffness of the supporting soil. The simplest design approach is that one in which the interaction of the underground structure with the surrounding soil is neglected. With this approach, first the soil deformation of free field are estimated, and then, the structure is designed to be adjusted to these deformations. Result is acceptable when the stiffness of both elements are similar. Contrarily, is necessary to consider the dynamic interaction effects due to the stiffness contrast between the soil and the structure. Zeevart (1983) proposed a practical method to compute seismic forces in shafts caused by the ground motion. However, the effect of frequency of excitation in the inertia of the soil is neglected. Also, seismic excitation is accounted for in approximated way by yielding the peak ground acceleration in the surface and estimating the lateral displacements configuration. Despite of these limitations, the method is very useful to show the importance of the supporting condition (articulation versus fixation) of the shaft.

In his work, Zeevaert (1983) proposes a layered media composed by 8 layers, with dominant period Ts=0.95 s. In this medium there is a shaft with 2 m radius and 16 m length connected in its base to a tunnel modeled as a rotational spring. For a 1 m/s2 acceleration in the soil surface, he obtains shear force (Q_z) and bending moment (M_z) profiles. Table 1 contains dynamic soil parameters derived from Zeevaert stratigraphic model. Excitation was modeled with synthetic accelerograms that fulfill, in average, whit the uniform hazard spectrum for hill zone in the valley of Mexico, scale to produce 1 m/s2 in the surface of the soil. Parameters of the shaft are: Vs = 2200 m/s, ν=0.2, ζ=5% and γ=2.2 t/m^3. Figures 6 shows (A) relative displacements, (B) shear force and (C) bending moment for the three selected supporting conditions for the shaft: (top) Floating in the soft soil (16 m length), (middle) supported in the half space (17 m length) and (bottom) fixed in the half space (18 m length).

Table 1. Dynamic Properties Of The Stratigraphic Model Proposed By Zeevaert (1983).

Layer	Thickness (m)	Vs(1) (m/s)	$\gamma^{(2)}$ (t/m^3)	$\nu^{(3)}$	$\zeta^{(4)}$ %
1	2	41	1.75	0.45	5
2	2	48	1.70	0.45	5
3	2	57	1.80	0.45	5
4	2	57	1.80	0.45	5
5	2	65	1.85	0.45	5
6	2	65	1.85	0.45	5
7	2	80	1.85	0.45	5
8	3	80	1.85	0.45	5
Half space	∞	500	2.00	0.45	

(1) Shear wave velocity, (2) Volumetric weight, (3) Poisson ratio, (4) Damping

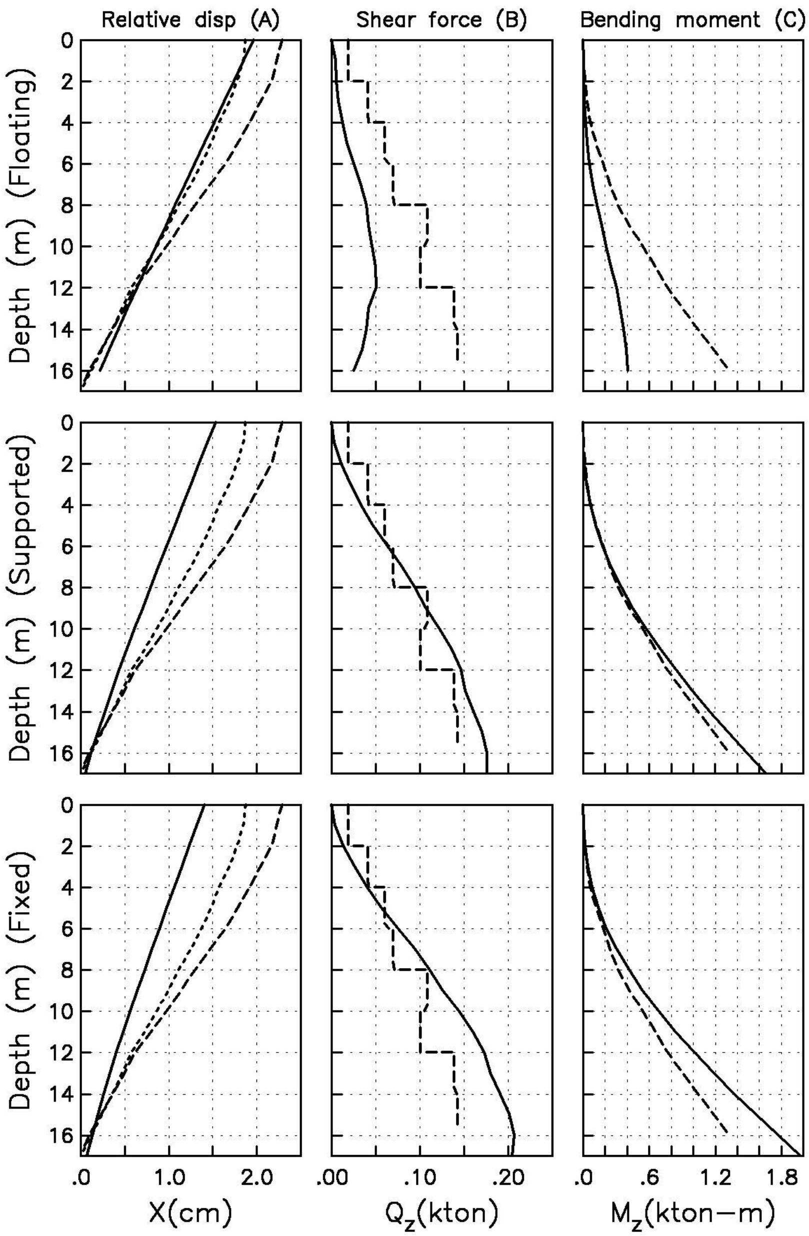

Figure 6. A) Relative displacements (right), B) Shear Force (center) and C) Bending Moment (left) for a floating (top), supported (middle) and fixed (bottom) shaft. Exact solution is shown with solid lines whereas Zeevaert solution is shown with dashed lines. Free field displacement (without SSI) is shown with dotted lines.

Relative displacements are shown at left in these figures. Exact solution of free field is indicated with dotted lines whereas Zeevaert approximation is indicated with dashed lines. Relative displacement of the shaft for each condition (floating, supported and fixed) is indicated with solid line. Note that Zeevaert approximation overestimates free field displacement in little more than 20%. Note that relative displacement of the shaft follows ground displacement for floating condition and also that its displacement is reduced when fixed condition.

Rigorous (solid lines) and Zeevaert approximation (dashed lines) shear forces are shown at the center of each row. Note that floating condition reduces substantially shear forces in comparison to supported condition (85%) and that Zeevaert solution provides values slightly smaller than the ones obtained with the supported condition (differences of 20% at the base). It has an increment of 16% in the fixed condition with respect to the supported condition.

Finally, rigorous (solid lines) and Zeevaert approximation (dashed lines) bending moments are shown at the right of each figure. Again, it is appraised that the floating shaft condition significantly reduces the moments with respect to the supported shaft condition (75%). As in shear forces, Zeevaert approximation yields bending moments that are slightly smaller than the ones obtained for the supported shaft condition (17%). An increment of 19% with respect to the supported shaft condition is had in the fixed shaft condition.

5. CONCLUSIONS

A modal superposition method for seismic analysis of floating flexible shafts has been presented. The method has been validated by comparison with theoretical results of rigid shafts fixed at their base (Veletsos and Younan, 1995, solution) and with numerical-approximated results for an embedded pilot in a two layer medium (Nicolau et al, 2001). The method also was validated with an approximated numerical result for an elastically supported shaft (Zeevaert, 1983). It was observed that the floating condition at the base has great influence in the magnitude and distribution of the soil actions. Excellent results were obtained in all these comparisons.

REFERENCES

Arias, A., Sánchez-Sesma, F.J. and Ovando-Shelley, E. (1981). A simplified elastic model for seismic analysis of earth-retaining structures with limited displacements. *Int. Conf. on Recent Advances in Geotechnical Earthquake Engineering and Soil Dynamics*. St. Louis, MO, 235-240.

Kausel, E., Roësset, J.M. and Wash, G. (1975). Dynamic analysis of footings on layered media. *Journal of the Engineering Mechanics Division, ASCE.* **101:5**, 679-693.

Kausel, E. and Roësset, J.M. (1975). Dynamic stiffness of circular foundations. *Journal of the Engineering Mechanics Division, ASCE*. **101:EM12**, 771-785.

Kausel, E. and Roësset, J.M. (1977). Semianalytic hyperelement for layered strata. *Journal of the Engineering Mechanics Division, ASCE.* **103:4**, 569-588.

Lysmer, J. and Drake, L.A. (1972). A finite element method for seismology. Methods in Computational Physics. Advances in Research and Applications, Ed. B A Bolt, Vol. 11: Surface Waves and Earth Oscillations, Academic Press.

Lysmer, J. and Waas, G. (1972). Shear waves in plane infinite structures. *Journal of the Engineering Mechanics Division, ASCE***. 98:1**, 85-105.

Nicolau, S., Mylonakis, G., Gazetas, G. and Tazoh, T. (2001). Kinematic pile bending during earthquakes: analysis and field measurements. *Géotechnique*, **51:5**, 425-440.

Tajimi, H. (1969). Dynamic analysis of a structure embedded in an elastic stratum. *Fourth World Conference on Earthquake Engineering*. Santiago, Chile, 53-69.

Tassoulas, J.L. and Kausel, E. (1983). Elements for the numerical analysis of wave motion in layered media. *International Journal for Numerical Methods in Engineering*. **19:7**, 1005-1032.

Veletsos, A.S. and Younan, A.H. (1994). Dynamic soil pressures on rigid cylindrical vaults. *Earthquake Engineering and Structural Dynamics*. **23:6**, 645-669.

Veletsos, A.S. and Younan, A.H. (1995). Dynamic modeling and response of rigid embedded cylinders. *Journal of Engineering Mechanics, ASCE*. **121:9**, 1026-1035.

Zeevaert, L. (1983). Lumbrera sujeta a la acción sísmica. *VI Congreso Nacional de Ingeniería Sísmica*. Puebla, México, 431-440.